Electronic Supporting Information

Secondary Organic Aerosol Formation from Linalool-Derived Criegee Intermediates: Mechanistic Insights into Criegee-Carbonyl Cycloadditions and Atmospheric Implications

Wai-Cha Chau,[a] Jocelyn Solorza,[a] Dariela Nuñez[a,b], César Barrales-Martínez,[c*] Rocío Durán[a,b*]
E-mail: rbduran@ucsc.cl and cbarrales@ubiobio.cl

[a]*Departamento de Química Ambiental, Facultad de Ciencias, Universidad Católica de la Santísima Concepción, 4090541 Concepción, Chile.*
[b]*Centro de Investigación en Biodiversidad y Ambientes Sustentables (CIBAS), Universidad Católica de la Santísima Concepción, Concepción, Chile*
[c]*Departamento de Química, Facultad de Ciencias, Universidad del Bío-Bío, Avenida Collao 1202, Concepción 4051381, Chile.*

Content

1. Computational details

1.1. Electronic structure calculations

Quantum chemistry calculations were carried out using DFT, which incorporates the effects of electronic exchange and correlation in the molecular systems analyzed. The long-range corrected hybrid method ωB97X-D[1,2] with the def2-TZVP[3] basis set was employed, as this methodology has been previously validated by our research group.[4] DFT calculations were performed using the Gaussian 16 [5] software. The stability of the wave function (WF) was tested by applying the stable=opt option in Gaussian 16, with all systems showing stable wave functions under the perturbations considered. A harmonic vibrational analysis was conducted to ensure that both the reactants and products corresponded to minimum on the potential energy surface (PES), and to identify the transition state (TS) as a first-order saddle point with a single imaginary frequency. DFT-based global and local reactivity descriptors were obtained using the operational formulas proposed by Parr et al.[6] In this regard, the Fukui function was calculated as an electron density difference: $f^-(r) = \rho^N(r) - \rho^{N-1}(r)$ and $f^+(r) = \rho^{N+1}(r) - \rho^N(r)$. To obtain the condensed Fukui function for atoms, $f^{\pm}(r)$ was integrated over the atomic basins provided by the topological analysis of electron density in the reference system, such that $f_A^{\pm} = \int_{\Omega_A} f^{\pm}(r)dr$, where W_A represents the spatial atomic domain of atom A. The integration of $f^{\pm}(r)$ was performed using the Multiwfn 3.5[7] program. Lastly, rate constants were determined using conventional transition state theory (TST).[8] Electronic energies entering the kinetic calculations were refined by single-point calculations at the DLPNO-CCSD(T)-F12[59]/cc-pVDZ-F12 level of theory. Rate constants were computed using the KiSThelP program,[9] where quantum tunneling effects were included through Wigner corrections in all cases. To assess the reliability of the adopted kinetic protocol, benchmark calculations were performed for representative Criegee intermediate reactions with water and formaldehyde previously investigated by Truhlar and co-workers using high-level theoretical methods.[61,62] The rate constants obtained with the present approach reproduce the reference values within the same order of magnitude for all benchmark reactions, with the largest deviation of CI + water reaction being approximately a factor of 0.4, which lies within the expected uncertainty range for atmospheric kinetic calculations (see Table S1 for more details).

1.2. Simulation of self-aggregation of small molecules at low density

The kinetically and thermodynamically favored SOAs were simulated individually in 300 Å × 300 Å × 300 Å cubic boxes. The initial coordinates were generated using the Packmol software.[10] Within each box, 300 molecules of each compound were distributed in a centered 100 Å sphere, separated by at least 3 Å. The environment was supplemented with representative atmospheric gases (N_2, O_2, and Ar) and 25 water molecules to represent low-humidity conditions. Partial charges for the SOAs were derived using the RESP method,[11] based on electrostatic potential calculations performed with Gaussian 16 at the ωB97X-D/def2-TZVP level of theory. Molecular topologies were generated using Antechamber and Parmchk2 from the AmberTools24 suite with the GAFF force field.[12,13] Water molecules were modeled using the TIP3P model,[14] while parameters for N_2, O_2, and Ar

were adopted from literature sources.[15,16] The systems were energy-minimized in three consecutive stages: (i) applying positional restraints of 10 kcal mol^{-1} $Å^{-2}$ on the SOA atoms, (ii) reducing the restraints to 3 kcal mol^{-1} $Å^{-2}$, and (iii) performing an unrestrained minimization. Each stage consisted of 5000 cycles of steepest descent followed by 5000 cycles of conjugate gradient minimization. Subsequent simulations were carried out in Amber24 using pmemd.cuda under NVT conditions.[17,18] The molecular dynamics protocol included four steps: heating from 10 K to 150 K with restraints of 10 kcal mol^{-1} $Å^{-2}$, heating from 150 K to 243 K with restraints reduced to 5 kcal mol^{-1} $Å^{-2}$), free equilibrium at 243 K with no restraints, dt = 2 fs, and production for 100 ns at 243 K. A Langevin thermostat with g = 2 ps^{-1}, a 10 Å cutoff for nonbonding interactions, and wrapped coordinates (iwrap=1) was employed.

The center of mass of each SOA was calculated in all frames of the trajectory. Hierarchical clustering was applied to the last frame with a distance criterion of 4.0 Å between centers of mass. Persistent clusters were identified, their structures extracted, and their temporal evolution analyzed. The NVT ensemble was selected to maintain constant temperature and volume, ensuring fixed supersaturation and boundary conditions during cluster formation. This approach is widely applied in nucleation studies, in condensed and vapor phases.[19–21] In NVT, the absence of volume fluctuations allows precise control of the thermodynamic state and facilitates direct comparisons between systems. However, its closed nature inherently reduces the number of free monomers over time, leading to an apparent stationary phase in cluster growth that reflects depletion effects rather than a true steady state, in contrast to open atmospheric conditions. It has been previously pointed out that the application of barostats in systems with low density or inhomogeneous distribution can induce artifacts, such as unphysical volume fluctuations or destabilization of incipient structures.[22] Consequently, the use of NVT allows for the preservation of a thermodynamically coherent environment and avoids external influences that could disrupt the observed molecular aggregation process.

2. Additional computational results

2.1 Comparative analysis of rate constant calculation

To further benchmark and validate the accuracy of our computational protocol, we reproduced well-established reference reactions involving Criegee intermediates for which reliable high-level theoretical data are available. Specifically, we recalculated the bimolecular reactions of CH_2OO, syn-CH_3CHOO, and anti-CH_3CHOO with as well as the CH_2OO + HCHO reaction.[61,62] These reactions were chosen because they represent prototypical Criegee intermediate processes and have been extensively characterized using high-level electronic structure methods. The comparison between our calculated rate constants and the reference values is summarized in Table S1. In all cases, the rate constants obtained with our model fall within the same order of magnitude as the benchmark data. The largest deviation corresponds to the CH_2OO + HCHO reaction (6.20×10^{-11} vs. 1.04×10^{-11} cm³ molecule^{-1} s^{-1}), whereas for water-involved reactions the largest deviation was found to be by a factor of 0.4 (Syn + H_2O). These results provide strong support for the reliability of the present ωB97X-D/def2-TZVP//DLPNO-CCSD(T)-F12/cc-pVDZ-F12 + TST/Wigner protocol in predicting rate constants for Criegee intermediate-driven atmospheric reactions.

Table S1. Rate constants calculated at the ωB97X-D/def2-TZVP//DLPNO-CCSD(T)-F12/cc-pVDZ-F12 level of theory using TST with Wigner tunneling corrections, compared with reference values reported by Truhlar and co-workers. All values are calculated at 298 K and are in cm^3 molecules^{-1} s^{-1}.

Reaction	k_{ref}	k_{calc}	k_{calc}/k_{ref}
CH_2OO + H_2O	2.41×10^{-16}	1.69×10^{-16}	0.7
***Syn*-CH_3CHOO + H_2O**	1.90×10^{-19}	7.70×10^{-20}	0.4
***Anti*-CH_3CHOO + H_2O**	5.21×10^{-15}	3.04×10^{-15}	0.6
CH_2OO + HCHO	6.20×10^{-11}	1.04×10^{-11}	0.2

2.2 Nucleation capacity of cloud condensation nuclei precursors (CCN) by dynamics simulations

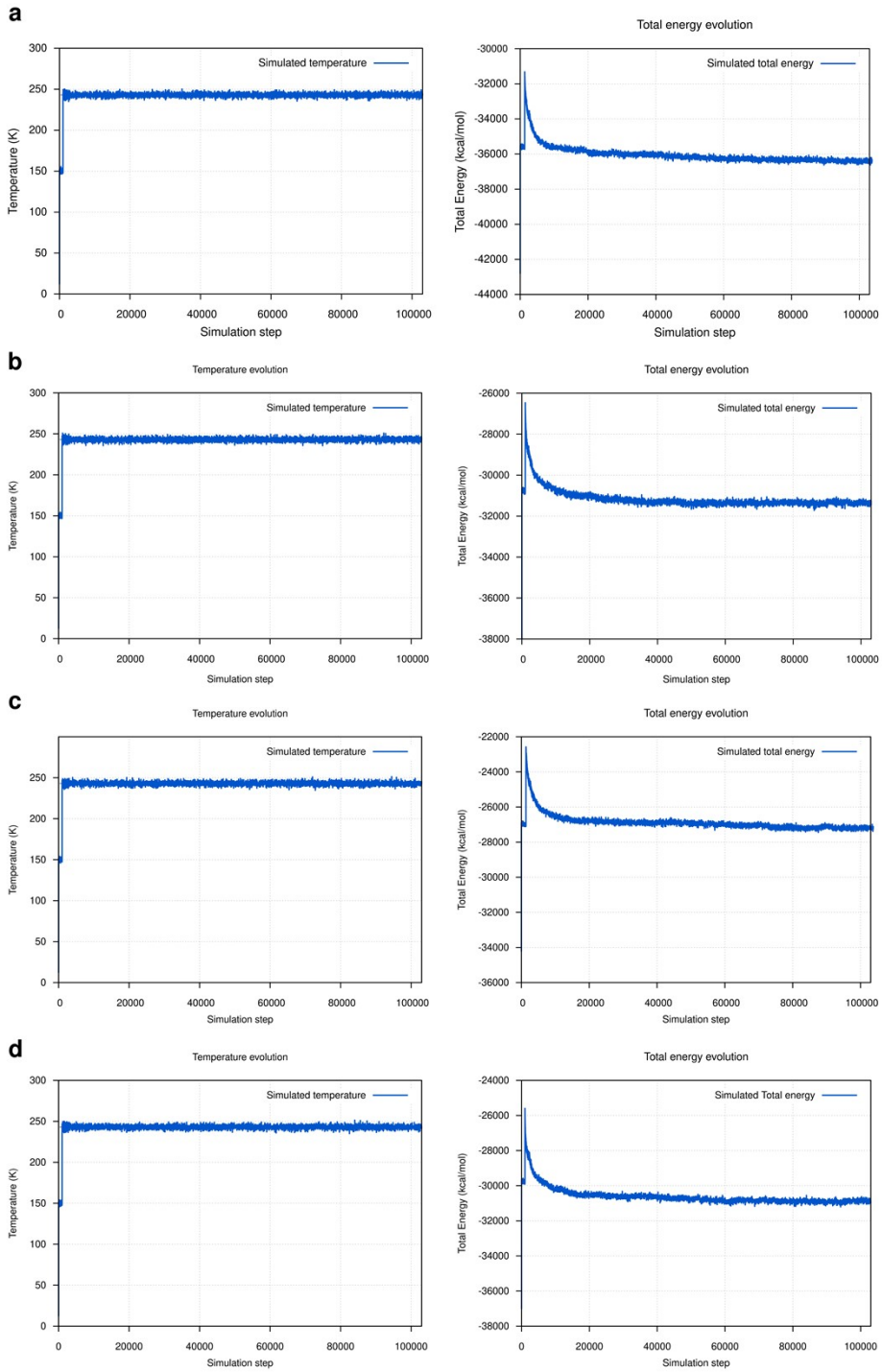

Figure S1: Shows the thermal and energy evolution of the simulated systems. The left panel illustrates the evolution of temperature, while the right panel displays the total energy for systems P1 (a), P2 (b), P5 (c), and P6 (d) throughout the simulations. Each profile covers the heating steps during the pre-production phase and

continues up to 100 ns of production. The early stabilization of both total energy and temperature indicates that the system is balanced, making it suitable for subsequent analysis of aggregation and condensation.

3 References

1. Y.-S. Lin, G.-D. Li, S.-P. Mao and J.-D. Chai, Long-range corrected hybrid density functionals with improved dispersion corrections, *J. Chem. Theory Comput*., 2013, 9, 263–272.

2. J.-D. Chai and M. Head-Gordon, Long-range corrected hybrid density functionals with damped atom–atom dispersion corrections, *Phys. Chem. Chem. Phys*., 2008, 10, 6615–6620.

3. F. Weigend and R. Ahlrichs, Balanced basis sets of split valence, triple zeta valence and quadruple zeta valence quality for H to Rn: design and assessment of accuracy, *Phys. Chem. Chem. Phys*., 2005, 7, 3297–3305.

4. R. Durán, C. Barrales-Martínez, J. Solorza and J. Alzate-Morales, Computational study of the 1,3-dipolar cycloaddition between Criegee intermediates and linalool: atmospheric implications, *J. Phys. Chem. A*, 2025, 129, 1099–1115.

5. M. J. Frisch, G. W. Trucks, H. B. Schlegel, G. E. Scuseria, M. A. Robb, J. R. Cheeseman, G. Scalmani, V. Barone, G. A. Petersson, H. Nakatsuji, X. Li, M. Caricato, A. V. Marenich, J. Bloino, B. G. Janesko, R. Gomperts, B. Mennucci, H. P. Hratchian, J. V. Ortiz, A. F. Izmaylov, J. L. Sonnenberg, D. Williams-Young, F. Ding, F. Lipparini, F. Egidi, J. Goings, B. Peng, A. Petrone, T. Henderson, D. Ranasinghe, V. G. Zakrzewski, J. Gao, N. Rega, G. Zheng, W. Liang, M. Hada, M. Ehara, K. Toyota, R. Fukuda, J. Hasegawa, M. Ishida, T. Nakajima, Y. Honda, O. Kitao, H. Nakai, T. Vreven, K. Throssell, J. A. Montgomery Jr., J. E. Peralta, F. Ogliaro, M. J. Bearpark, J. J. Heyd, E. N. Brothers, K. N. Kudin, V. N. Staroverov, T. A. Keith, R. Kobayashi, J. Normand, K. Raghavachari, A. P. Rendell, J. C. Burant, S. S. Iyengar, J. Tomasi, M. Cossi, J. M. Millam, M. Klene, C. Adamo, R. Cammi, J. W. Ochterski, K. Morokuma, O. Farkas, J. B. Foresman and D. J. Fox, Gaussian 16, Revision B.01, Gaussian, Inc., Wallingford CT, 2016.

6. R. G. Parr and W. Yang, Density-Functional Theory of Atoms and Molecules, Oxford University Press, New York, 1989.

7. T. Lu and F. Chen, Multiwfn: a multifunctional wavefunction analyzer, *J. Comput. Chem.*, 2012, 33, 580–592.

8. D. G. Truhlar, B. C. Garrett and S. J. Klippenstein, Current status of transition-state theory, *J. Phys. Chem*., 1996, 100, 12771–12800.

9. S. Canneaux, F. Bohr and E. Henon, KiSThelP: a program to predict thermodynamic properties and rate constants from quantum chemistry results, *J. Comput. Chem*., 2014, 35, 82–93.

10. L. Martínez, R. Andrade, E. G. Birgin and J. M. Martínez, PACKMOL: a package for building initial configurations for molecular dynamics simulations, *J. Comput. Chem.*, 2009, 30, 2157–2164.

11. C. I. Bayly, P. Cieplak, W. Cornell and P. A. Kollman, A well-behaved electrostatic potential based method using charge restraints for deriving atomic charges: the RESP model, *J. Phys. Chem*., 1993, 97, 10269–10280.

12. J. Wang, W. Wang, P. A. Kollman and D. A. Case, Automatic atom type and bond type perception in molecular mechanical calculations, *J. Mol. Graph. Model*., 2006, 25, 247–260.

13. J. Wang, R. M. Wolf, J. W. Caldwell, P. A. Kollman and D. A. Case, Development and testing of a general AMBER force field, *J. Comput. Chem.,* 2004, 25, 1157–1174.

14. W. L. Jorgensen, J. Chandrasekhar, J. D. Madura, R. W. Impey and M. L. Klein, Comparison of simple potential functions for simulating liquid water, *J. Chem. Phys.,* 1983, 79, 926–935.

15. G. Maitland, M. Rigby, E. Smith, W. Wakeham and D. Henderson, Intermolecular forces: their origin and determination, *Phys. Today,* 1983, 36, 57–58.

16. S. Wang, K. Hou and H. Heinz, Accurate and compatible force fields for molecular oxygen, nitrogen, and hydrogen to simulate gases, electrolytes, and heterogeneous interfaces, *J. Chem. Theory Comput*., 2021, 17, 5198–5213.

17. R. Salomon-Ferrer, A. W. Götz, D. Poole, S. Le Grand and R. C. Walker, Routine microsecond molecular dynamics simulations with AMBER on GPUs. 2. Explicit solvent particle mesh Ewald, *J. Chem. Theory Comput*., 2013, 9, 3878–3888.

18. D. A. Case, H. M. Aktulga, K. Belfon, I. Y. Ben-Shalom, J. T. Berryman, S. R. Brozell, D. S. Cerutti, T. E. Cheatham III, G. A. Cisneros, V. W. D. Cruzeiro, T. A. Darden, N. Forouzesh, G. Giambaşu, T. Giese, M. K. Gilson, H. Gohlke, A. W. Goetz, J. Harris, S. Izadi, S. A. Izmailov, K. Kasavajhala, M. C. Kaymak, E. King, A. Kovalenko, T. Kurtzman, T. S. Lee, P. Li, C. Lin, J. Liu, T. Luchko, R. Luo, M. Machado, V. Manathunga, K. M. Merz, Y. Miao, O. Mikhailovskii, G. Monard, H. Nguyen, K. A. O'Hearn, A. Onufriev, F. Pan, S. Pantano, R. Qi, A. Rahnamoun, D. R. Roe, A. Roitberg, C. Sagui, S. Schott-Verdugo, A. Shajan, J. Shen, C. L. Simmerling, N. R. Skrynnikov, J. Smith, J. Swails, R. C. Walker, J. Wang, H. Wei, X. Wu, Y. Wu, Y. Xue, D. M. York, S. Zhao, Q. Zhu and P. A. Kollman, Amber 2023, University of California, San Francisco, 2023.

19. S. Toxvaerd, Molecular-dynamics simulation of homogeneous nucleation in the vapor phase, *J. Chem. Phys*., 2001, 115, 8913–8920.

20. B. E. Wyslouzil and J. Wölk, Overview: homogeneous nucleation from the vapor phase—The experimental science*, J. Chem. Phys*., 2016, DOI:10.1063/1.4962283.

21. J. R. Espinosa, E. Sanz, C. Valeriani and C. Vega, Homogeneous ice nucleation evaluated for several water models*, J. Chem. Phys*., 2014, DOI:10.1063/1.4897524.

22. J. Diemand, R. Angélil, K. K. Tanaka and H. Tanaka, Large scale molecular dynamics simulations of homogeneous nucleation*, J. Chem. Phys*., 2013, DOI:10.1063/1.4818639.